Know Noise: Realistic Random Processes for Simulations

Robert Nachtrieb [1], Tom Fiddaman [2], Ron Suiter [2], Tom Erickson [3], Scott Johnson [4]
Affiliation: [1] MIT Sloan School, [2] Ventana Systems, [3] EERC, [4] UND

Abstract:
When the integration of renewable electrical generation with a distribution network is modeled, the random aspects of wind and solar power generation must be modeled correctly to make appropriate investment decisions, and to assure reliability. Supply must balance demand on a timescale of much less than one hour, and yet fluctuations in solar and wind can have correlations with timescales exceeding one month. As an example, we analyze hourly generation and demand in the Midcontinent Independent System Operator (MISO) region. After the periodic components are subtracted, solar photovoltaic can be modeled with a fractional Gaussian process, and wind generation and demand can be modeled with Markov–Gauss processes with timescales of one week and one month, respectively. We show the first-order "pink noise" approximation may produce misleading results. Supplemental material provides Vensim code for fractional Gaussian and fractional Brownian processes.

Introduction
A typical approach in time series analysis is to subtract the periodic and autoregressive components and to assume that the residual is described by a white noise process [Box, 2015]. Sterman correctly points out that it is necessary to model noise itself as a process with inertia, or memory, which a white noise process does not have [Sterman, 2000, Appendix B]. Mandelbrot was the first to show quantitatively that the assumption of a white noise process is often violated in physical systems: exhibit extreme events and sequences of values above or below the mean more often than would be expected from a Gaussian distribution [Mandelbrot, 1971, and references therein].

This paper demonstrates several common noise processes, including Gaussian, or white noise; Brownian; boxcar averaged Gaussian noise; Markov–Gauss, or pink noise; two-stage exponential filtered Gaussian noise; fractional Gaussian; and fractional Brownian. The paper compares the common noise processes through the lens of the power spectral density, derived from the fast Fourier transform, which makes it particularly easy to recognize periodic components of the signal that may be added to the noise. Supplemental material provides simulation code to generate and analyze the periodic and noise processes.

As a motivating example, we demonstrate the application of these techniques for the integration of renewable electrical generation in the Midcontinent Independent System Operator (MISO) region. [EIA 2021] Figure 1 shows the hourly production of electricity from solar photovoltaics in the MISO region. The full time series shows that generation is higher in the summer than it is in the winter. The increase in overall solar generation at the beginning of 2021 is due to an increase in generating capacity. From the sample inset, we can see that production of solar is higher during the day than at night, as expected.

In the absence of grid-scale energy storage, electrical supply must match electrical demand on an hour-by-hour basis. Renewable sources of electricity, such as solar photovoltaic (PV) and wind, typically have the lowest marginal cost and, therefore, are rarely curtailed. The merit-order effect [Sensfuß, 2008] explains why as capacity of solar PV and wind generation increase, it will be harder to match supply and demand without grid-scale energy storage. The need to match supply and demand on both short and long timescales is described by Ford. [Ford, 2018]

Figure 2 shows the Fourier power spectral density of the normalized solar supply. The most prominent feature of the solar power spectral density is the contribution from daily fundamental frequency and integer harmonics that together generate the typical waveform shown in the Figure 1 inset. In addition, there is a broad background noise, which can be seen decreasing inversely proportional to the frequency. Figure 2 shows the solar generation with the periodic components subtracted, leaving only the "random" portion.

Figure 3 shows the Fourier transform of the random component of solar PV production, both before and after the periodic components have been reduced. Comparison shows that the daily fundamental and harmonics have been reduced but not completely eliminated and the random component is more clearly visible. The 1/f frequency dependence is more clearly visualized once the periodic components have been reduced.

To model long-term balance between supply and demand, we need to model the long-term fluctuations of supply and demand. The total variation of supply and demand set the capacity requirements for electrical storage and determine the probability of curtailment or brownouts.

Examples of Noise Processes

Figure 4a shows an example of a synthetic, purely coherent signal: by construct, the signal that has no noise. The signal repeats every 24 hours and two pulses per day. Figures 4b and 4c show the power spectral density and phase angle of the Fourier transform of the signal, respectively. The line spectra in the power spectral density indicate the presence of periodic signals; the absence of randomness in the phase angle indicates that the signal is coherent. Figure 4b shows that the periodic signal with the lowest frequency, the fundamental, is once per day and that the other periodic signals are integer harmonics of the fundamental.

To generate the time series in Figure 4, we translate time into fractions of a day and use a Vensim lookup to reproduce the daily behavior. We will use a two-dimensional generalization of this approach later to represent the periodic components of PV electrical generation, wind generation, and electricity demand.

By contrast Figure 5a shows an example of Gaussian noise generated by the Vensim RANDOM NORMAL function. The time series in Figure 5a shows only the first 100 hours, but the complete time series extends to 10,000 hours. Figures 5b and 5c show the power spectral density and the phase angle of the Fourier transform, respectively. The mean power spectral density is independent of frequency. The true signature of a random signal is shown in Figure 5c: the phase angle is uniformly distributed over all angles, i.e. is incoherent.

Given how easy it is to generate a Gaussian noise signal, one might be tempted to use a Gaussian noise process to represent a random physical process. However, this will give results that may be inconsistent with physical evidence.

Specifically, the Gaussian process (also known as white noise) has higher power per unit frequency at high frequencies than most physical systems exhibit. A physical random system should be evaluated to determine the dependence of the power spectral density on frequency, which a faithful simulation will reproduce.

Figure 6 shows a system which produces a random signal with power spectral density that decreases with frequency. The causal diagram in the inset indicates that process input is a white noise signal, which is integrated without loss to produce the so-called Brownian noise signal (sometimes called a random walk). Figure 6a shows the original white noise signal in red and the Brownian noise signal in blue. Figure 6b shows the power spectral density of the Brownian noise process, which decreases with the inverse square of the frequency (red line). The phase angle portion of the Fourier transform is random and is not shown.

The Brownian noise process is said to have a perfect memory: every impulse from the white noise input is accumulated without loss. Figure 7 shows an example of a process with imperfect memory: a boxcar moving average. The averaging time in this example is set for 10 hours, which means the boxcar average remembers the signal perfectly for 10 hours and then completely loses any knowledge of the signal prior to 10 hours ago. In other words, only samples within the averaging time are retained to construct the boxcar average. Figure 7a shows the time series with the white noise input (red) and the boxcar moving average (blue); Figure 7b shows the power spectral density. For intervals longer than the averaging time (for frequencies lower than the inverse of the averaging time), the boxcar average has no memory, and the power spectral density is flat, like the Gaussian process.

For intervals shorter than the averaging time (frequencies higher than the inverse of the averaging time), the boxcar average power spectral density shows absorption-like artifacts introduced at harmonics of the inverse of the averaging time. Physical systems that do not actually exhibit these features would be poorly modeled by a boxcar average.

Figure 8 shows an example of an exponential moving average, with the averaging time set to 10 hours. Like the boxcar average, the system has no memory for frequencies lower than the inverse of the averaging time, and the power spectral distribution is flat, like the Gaussian process. For intervals shorter than the averaging time (frequencies higher than the inverse of the averaging time), the power spectral density decreases with the inverse square of the frequency. An exponential moving average can be thought of as a hybrid between a Gaussian process at low frequencies and a Brownian process at high frequencies, with the division between “low” and “high” frequency corresponding to the inverse of the averaging time. The exponential moving average of a white noise process is known as a Markov–Gauss process.

In Figure 9, we show a two-stage exponential moving average, using Vensim SMOOTH N and ORDER = 2. From Figure 9a we can see that the output of the process has even less variation than the output from a single-stage exponential process (Figure 8a). From Figure 9b, we see that the power spectral density decreases faster than the inverse cube of the frequency, the dotted red line. Theoretically, the two-stage exponential filter of a white noise process decays like the inverse fourth power of frequency above the cutoff frequency.

Until now we have shown how to generate processes that exhibit no decay with frequency (Gaussian) or decay with the inverse square of the frequency (Markov–Gauss), but what about a physical system whose signal decays *slower* than the inverse square, say like the inverse of the frequency? The power spectral distribution of solar PV (Figure 3) is a physical example of such a system. To model such a process, Figure 10 shows the causal diagram of a process model that can generate a so-called fractional Gaussian signal. This process was first described by Mandelbrot [1971] to model hydrological records. The fractional Gaussian signal is constructed as a superposition of Markov–Gaussian processes, with the correlation length and amplitude adjusted such that the decay of the power spectral density of the superposition matches the desired exponent alpha.

Figure 11 shows the example of a fractional Gaussian process, where the power spectral density decreases by one over the frequency, $1/f^a$, a = 1. A fractional Browning process is constructed by the integral of a fractional Gaussian process. See supplemental materials.

Figure 12 shows a superposition of the synthetic coherent and synthetic fractional Gaussian process. One can discern from the time series in Figure 12a that the original coherent signal has had a random component added to it. By simply looking at a short segment of the time series, it is impossible to identify the nature of the random component. However, by examining the power spectral density of a much larger sample, say 10,000 samples, it is possible to identify the periodic components and the random components. In this case, even with the presence of the periodic components in the power spectral density, it is possible to recognize that the power spectral density decays with the inverse of the frequency.

Application

Figures 13a and 13b show the periodic structure of the solar PV and wind electricity generation in the MISO region, respectively. The data exhibit daily and annual harmonics, which we estimate by averaging the generation for combination of hour of the day and month of the year, then dividing by the overall average. Rows represent month of the year, and columns represent hour of the day. The color shading helps to confirm that solar PV generation is higher (green) during the day than at night (of course) and higher during the summer than in the winter; periodic components of wind generation are higher during the winter and at night.

Figure 14 shows the periodic structure of electricity demand. Since behavior changes during the week, rows show each of the 168 hours in a week. Columns represent month of the year. It can be seen that periods of higher demand (green) occur during the day and during the Monday–Friday work week.

The periodic structure from Figures 13 and 14 can be subtracted from the original signal to produce a new signal that is more nearly “pure random” in that the periodic components of the power spectral density have been reduced. Figure 15 shows the power spectral density of wind generation (top) and demand (bottom), both before (left) and after (right) subtraction of the periodic components. In particular, weekly harmonics and weekly and daily beat harmonics that can be observed in the demand power spectral density are mostly removed by the subtraction procedure. The remaining power spectral densities appear well-represented by Markov–Gauss processes with averaging times of 1 week and 1 month, respectively.

References

Box, George EP, Gwilym M. Jenkins, Gregory C. Reinsel, and Greta M. Ljung. *Time series analysis: forecasting and control*. John Wiley & Sons, 2015.

Ford, Andrew. "Simulating systems with fast and slow dynamics: lessons from the electric power industry." *System Dynamics Review* 34, no. 1-2 (2018): 222-254.

Mandelbrot, Benoit B. "A fast fractional Gaussian noise generator." *Water Resources Research* 7, no. 3 (1971): 543–553.

Sensfuß, Frank, Mario Ragwitz, and Massimo Genoese. "The merit-order effect: A detailed analysis of the price effect of renewable electricity generation on spot market prices in Germany." *Energy Policy* 36, no. 8 (2008): 3086–3094.

Sterman, John. *Business dynamics*. Irwin/McGraw-Hill, 2000.

US Energy Information Agency. Hourly load and generation data retrieved 2021-03-25, available at https://www.eia.gov/opendata/qb.php?category=2123635.

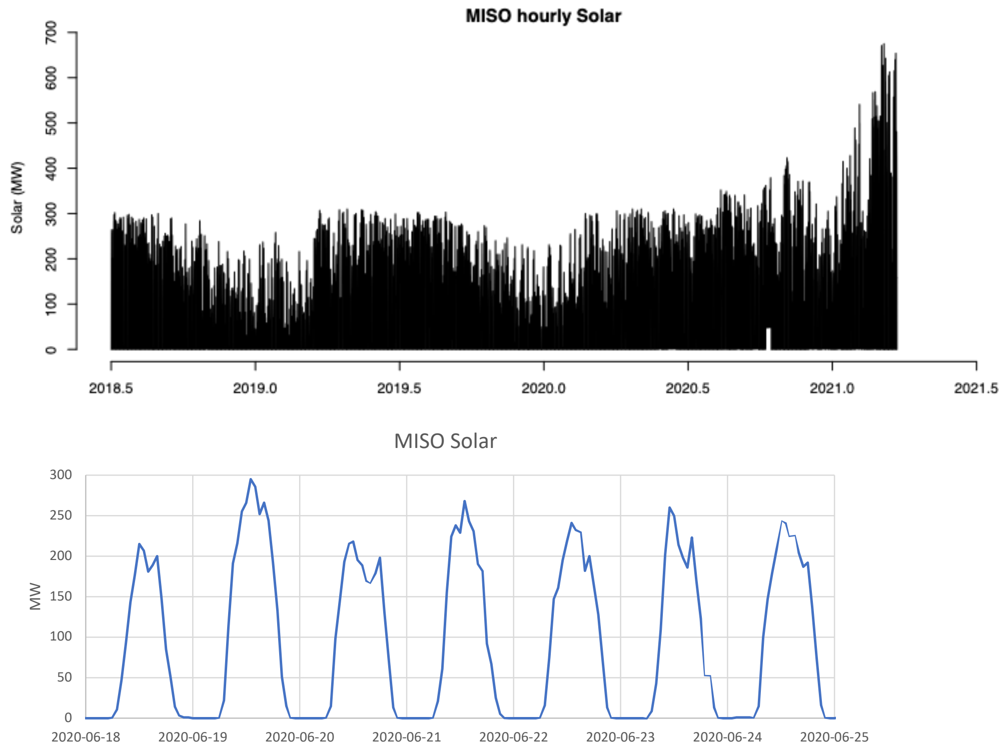

Figure 1 Top: hourly electrical generation from solar photovoltaics in the MISO region from July, 2018 through February, 2021. Inset: solar PV electrical generation for one week during the middle of 2020. Increase at the beginning of 2021 is the result of increasing generation capacity.

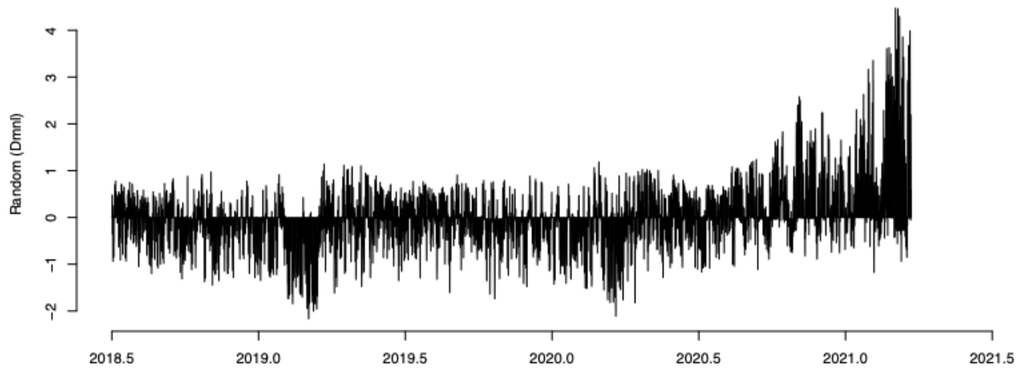

Figure 2 Hourly electrical generation from solar photovoltaics, offset and normalized to have zero mean and unit standard deviation.

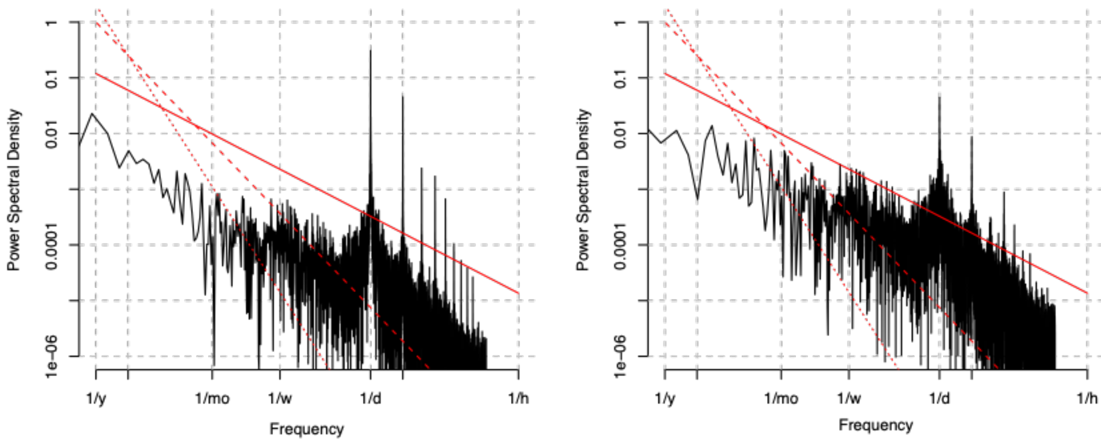

Figure 3 Solar photovoltaic power spectral density. Solid reference line ~ 1/f, dashed line ~1/f^2, and dotted line ~1/f^3.

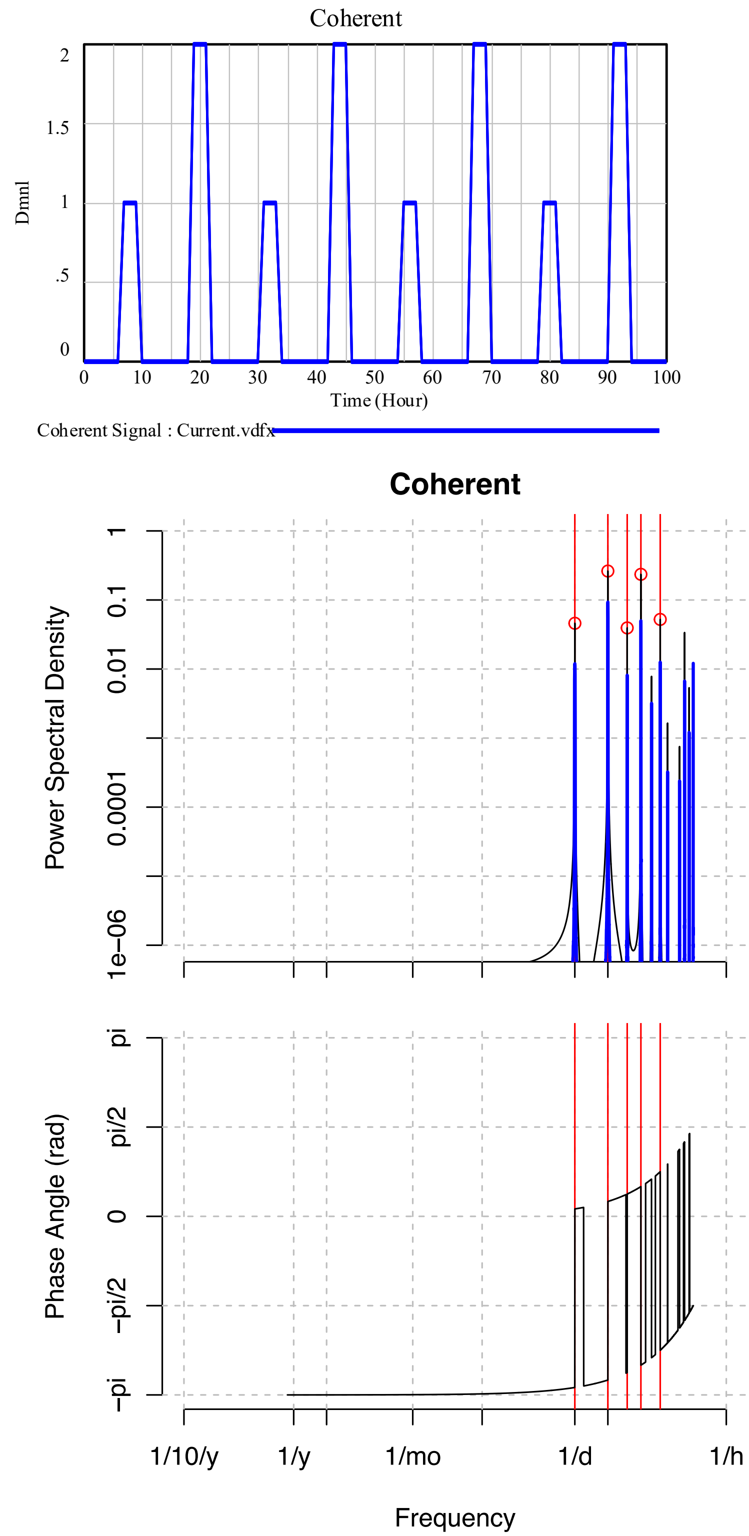

Figure 4 Top: Synthetic hourly time series, showing first 100 samples of 10,000 total points. Middle: power spectral density portion of Fourier transform showing daily fundamental frequency with integral harmonics. Bottom: phase angle portion of the Fourier transform, showing coherent structure.

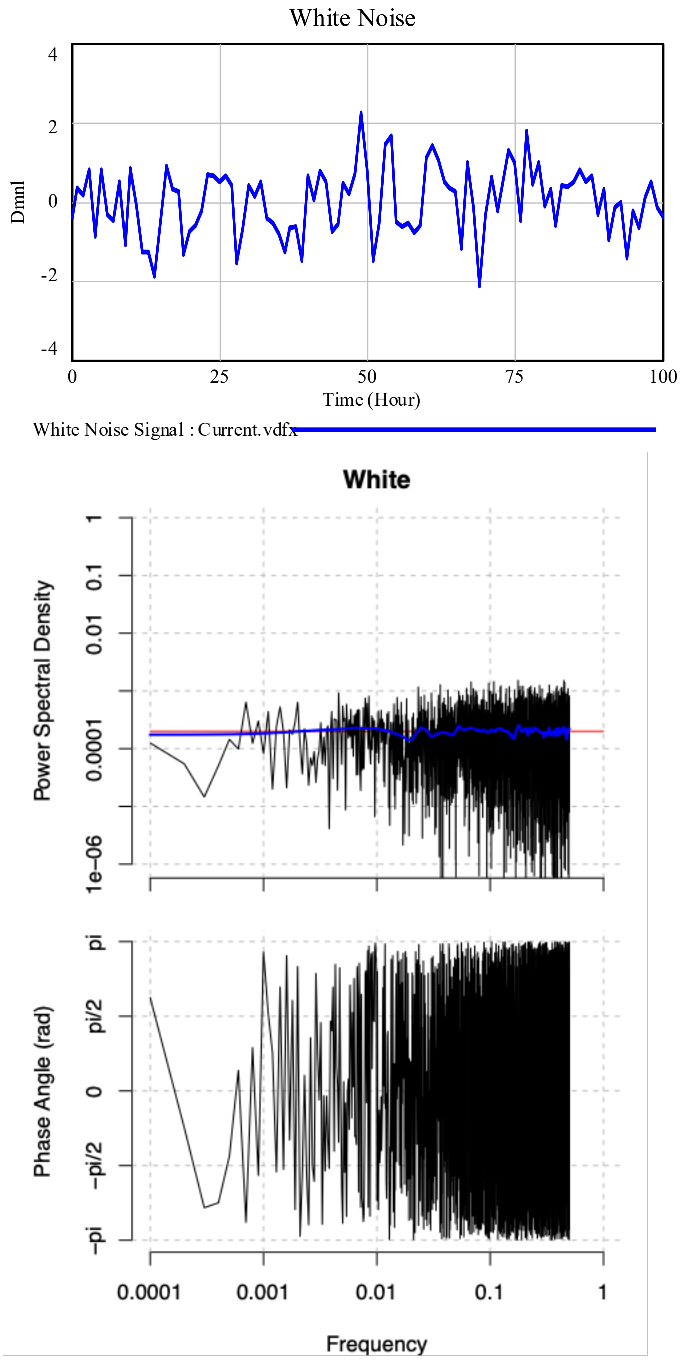

Figure 5 Gaussian noise process generating hourly data, showing first 100 samples of 10,000 total points. Middle: power spectral density. Spectral density is independent of frequency, which is a characteristic of a white noise process. Bottom: phase angle of the Fourier transform. The phase angle is uniformly distributed over all frequencies, i.e. is incoherent, which is characteristic of an random process.

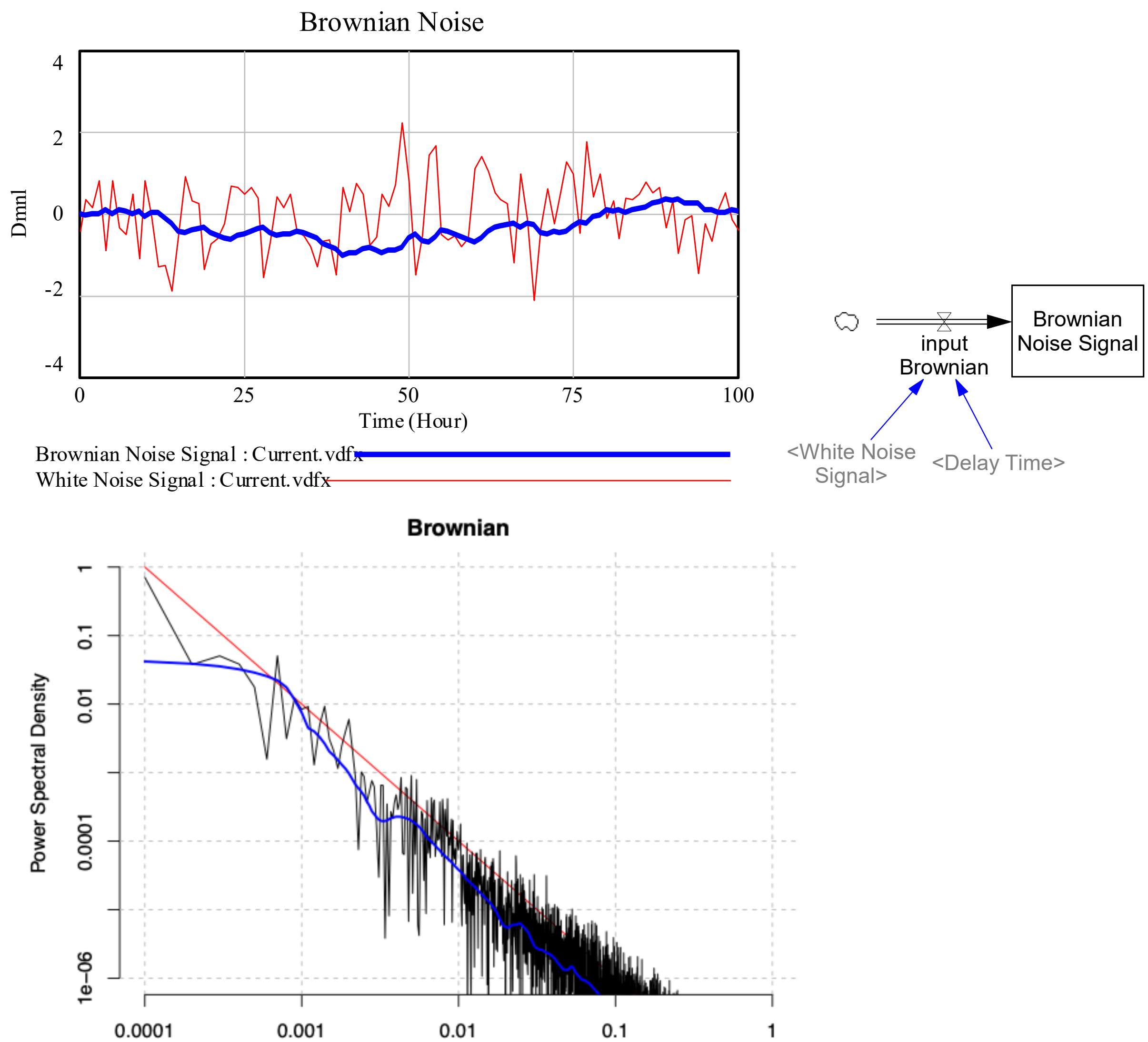

Figure 6 Brownian noise process generating hourly data, showing first 100 samples of 10,000 total points. The red trace is the white noise signal input, thick blue line is the Brownian process output. Bottom: power spectral density, showing a decreasing amplitude with frequency. Red line is proportional to inverse square of frequency.

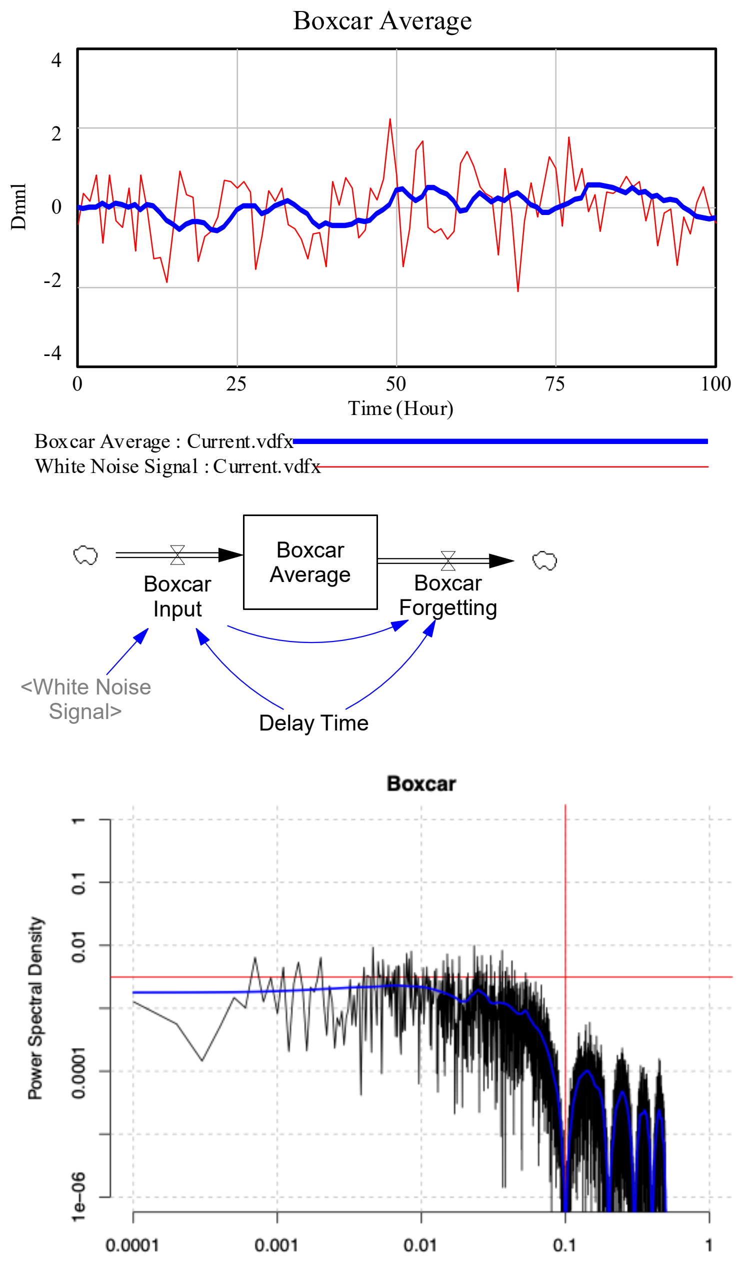

Figure 7 Box car average of a white noise hourly process, with ten averaging time. Top: first 100 samples of 10,000 total points. Red line is the white noise input, and solid blue line is the box car average output. Middle: causal loop diagram of the boxcar average process. Bottom: power spectral density of the box car average of white noise process. For timescales longer than the delay time (frequencies lower than the inverse of the delay time) the power spectral density is independent or frequency, indicating it has no long-term memory. For timescales shorter than the delay time (frequencies higher than the inverse delay time), the power spectral density amplitude decreases. Absorption spectra at harmonics of the inverse delay time are not commonly observed for physical processes.

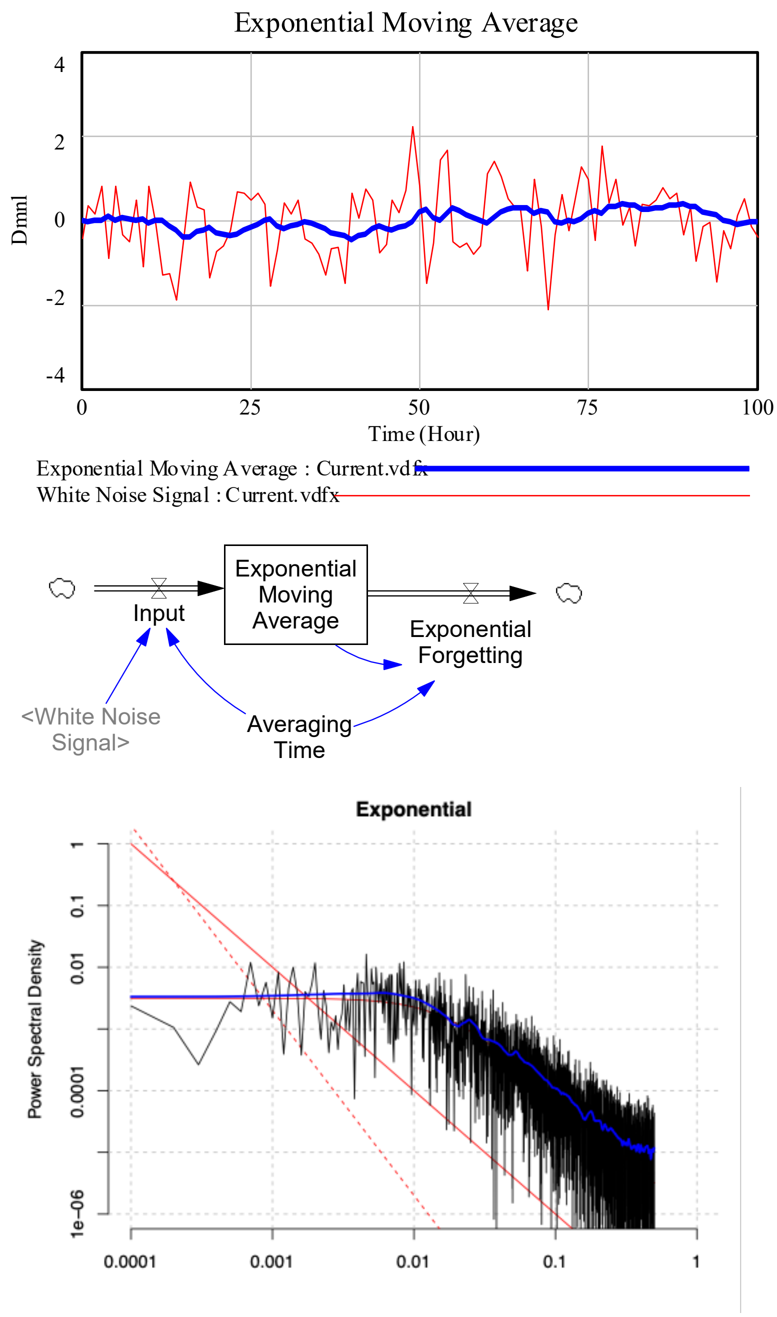

Figure 8 Exponential moving average of a white noise hourly process, also known as Markov-Gauss process. Top: red line is white noise input to Markov-Gauss process, solid blue line represents the Markov-Gauss process output, with averaging time set to 10 hours. Middle: causal loop diagram to construct the Markov-Gauss process. Bottom: power spectral density of Markov-Gauss process. For timescales longer than the inverse averaging time, power spectral density is independent of frequency, like a white noise process. For timescales shorter than the averaging time (frequency higher than the inverse averaging time), power spectral distribution of exponential moving average decreases with inverse square of the frequency. Solid and dashed red lines is proportional to inverse square and to inverse cube of frequency, respectively.

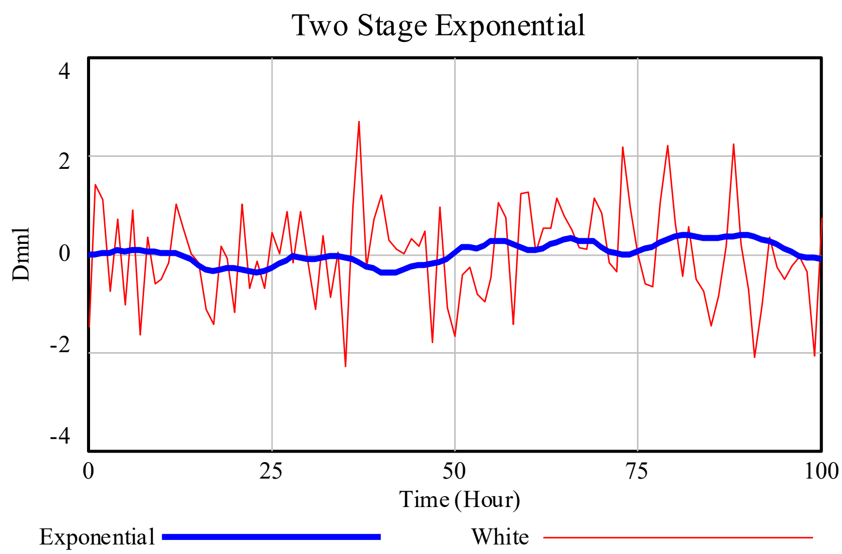

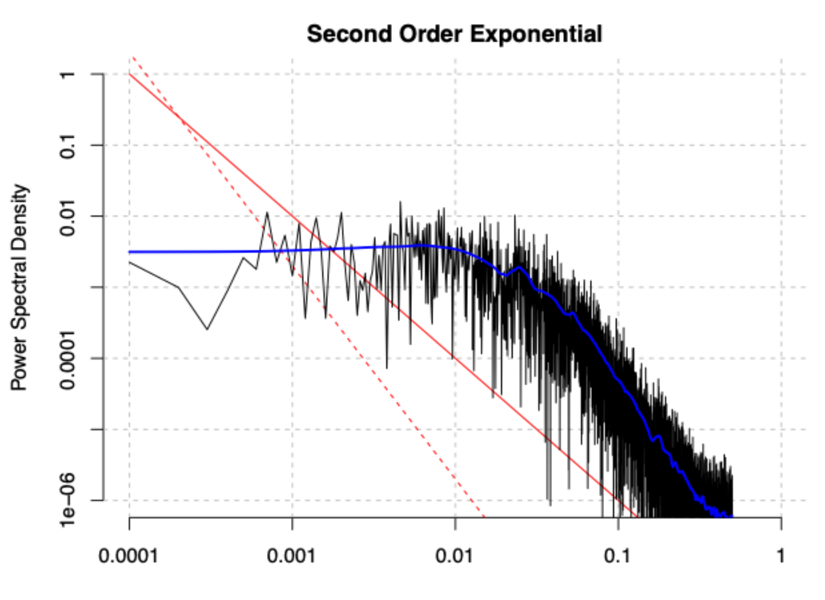

Figure 9 Two-stage exponential smoothing of white noise hourly process, with averaging time set to 10 hours. For timescales longer than the averaging time (frequencies lower than the inverse averaging time), the power spectral distribution is independent of frequency. For timescales shorter than the averaging time (frequencies higher than the inverse averaging time), power spectral density decreases faster than the inverse cube of the frequency (dashed red line). Theory indicates second order exponential filtering of Gaussian process should decrease with inverse fourth power of frequency at frequencies above inverse of averaging time.

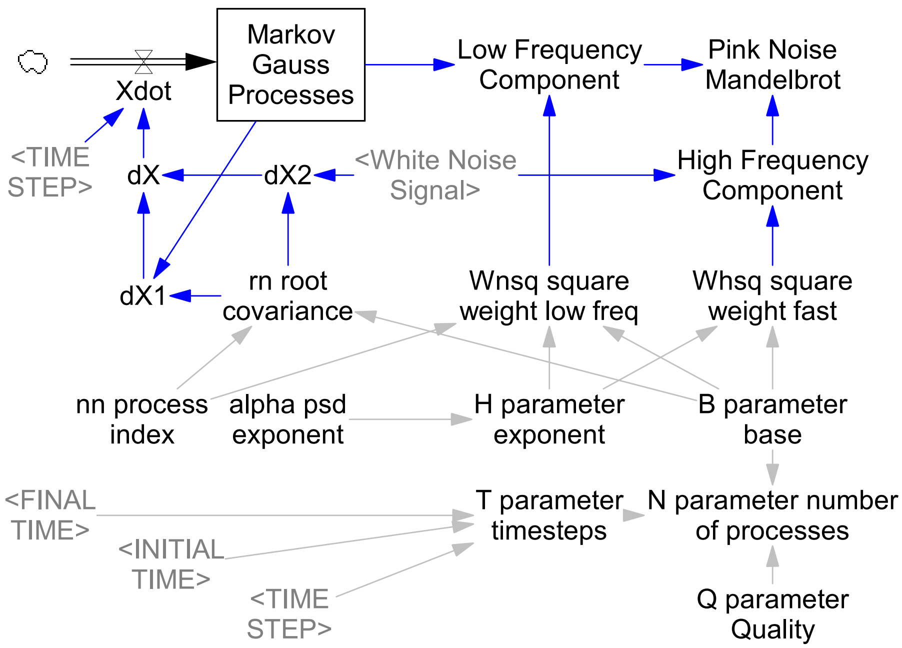

Figure 10 Causal diagram of a fractional Gaussian process described by Mandelbrot. [Mandelbrot, 1971]. Process consists of a superposition of independent Markov-Gaussian processes with correlation times and amplitudes adjusted such that resulting power spectral distribution decreases with frequency proportional to inverse power alpha.

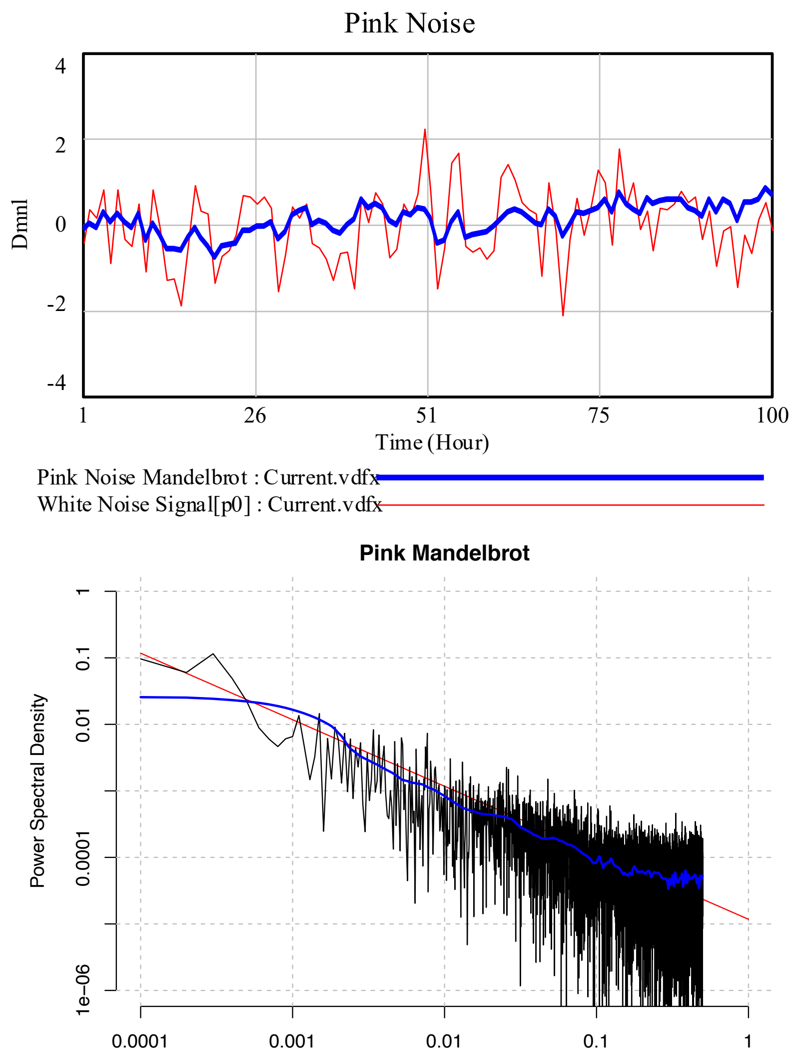

Figure 11 Output of a fractional Gaussian process, with inverse frequency power alpha corresponds to one. Top: red line is one of the input white noise signals, and solid blue line is output of the fractional Gaussian process. First 100 samples of 10,000 points total. Bottom: power spectral density showing decline with frequency proportional to inverse frequency.

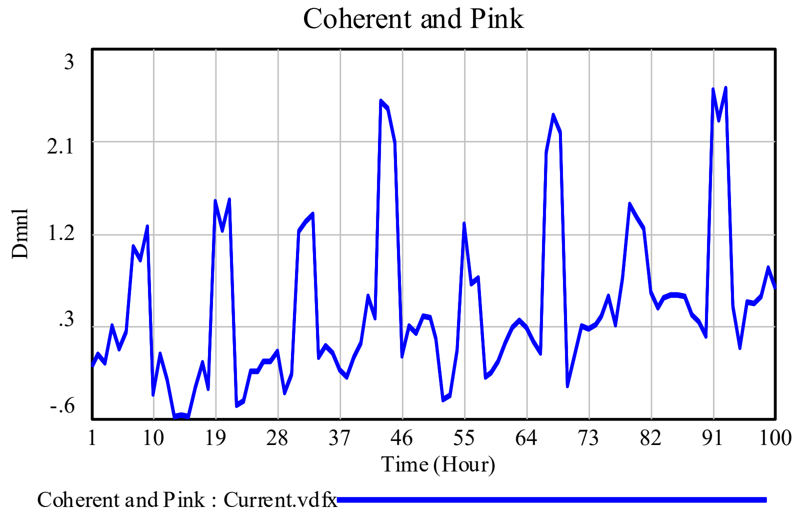

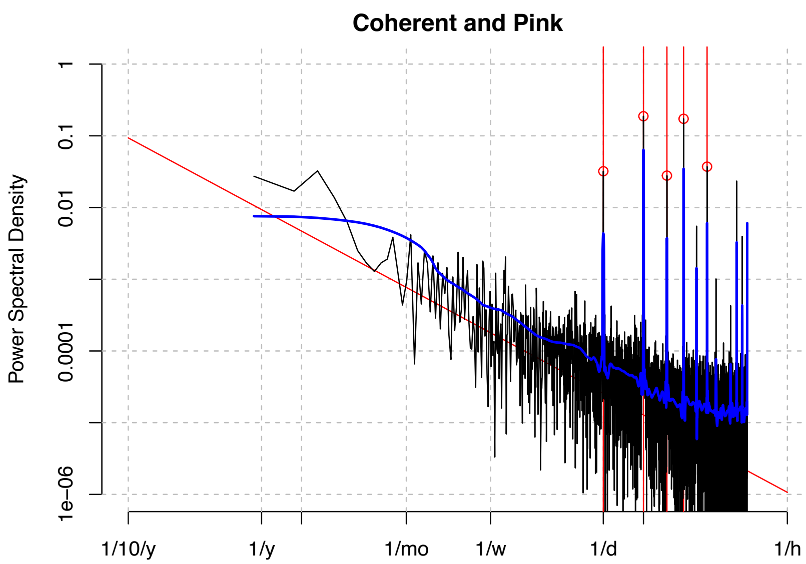

Figure 12 Superposition of a coherent and fractional Gaussian process with alpha corresponding to one. First 100 samples of 10,000 point total. Bottom: power spectral density of mixture of coherent and fractional Gaussian process. The resonances corresponding to harmonics of the fundamental daily period are clearly visible, superimposed on the background of inverse frequency random noise.

Average of c Columr																								
Month	**0**	**1**	**2**	**3**	**4**	**5**	**6**	**7**	**8**	**9**	**10**	**11**	**12**	**13**	**14**	**15**	**16**	**17**	**18**	**19**	**20**	**21**	**22**	**23**
1	0.00	0.00	0.00	0.00	0.00	0.00	0.00	0.00	0.07	0.65	1.59	2.21	2.48	2.52	2.43	2.15	1.48	0.46	0.02	0.00	0.00	0.00	0.00	0.00
2	0.01	0.01	0.01	0.00	0.00	0.01	0.01	0.01	0.27	1.22	2.18	2.68	2.87	2.89	2.83	2.73	2.24	1.12	0.18	0.01	0.01	0.01	0.01	0.01
3	0.00	0.00	0.00	0.00	0.00	0.00	0.00	0.02	0.48	1.75	2.71	3.25	3.50	3.57	3.61	3.53	3.22	2.53	1.35	0.41	0.02	0.00	0.00	0.00
4	0.00	-	0.00	0.00	0.00	0.00	0.00	0.02	0.47	1.44	2.20	2.62	2.84	2.92	2.86	2.90	2.68	2.38	1.80	0.98	0.19	0.00	0.00	0.00
5	0.00	0.00	0.00	0.00	0.00	0.00	0.00	0.15	0.90	1.74	2.32	2.78	2.98	2.99	3.02	3.02	2.90	2.55	2.05	1.31	0.43	0.04	0.00	0.00
6	0.00	0.00	0.00	0.00	0.00	0.00	0.01	0.26	1.09	1.89	2.50	3.00	3.21	3.25	3.27	3.17	2.99	2.66	2.13	1.45	0.70	0.13	0.00	0.00
7	0.00	0.00	0.00	0.00	0.00	0.00	0.00	0.15	0.90	1.81	2.47	2.94	3.21	3.23	3.26	3.19	3.00	2.68	2.14	1.50	0.67	0.10	0.00	-
8	0.00	0.00	0.00	0.00	0.00	0.00	0.00	0.03	0.56	1.67	2.52	3.04	3.30	3.39	3.42	3.28	3.12	2.75	2.15	1.23	0.31	0.02	0.00	0.00
9	0.00	0.00	0.00	0.00	0.00	0.00	0.00	0.00	0.23	1.20	2.12	2.68	3.00	2.97	2.92	2.89	2.68	2.24	1.51	0.51	0.03	0.00	0.00	0.00
10	0.05	0.05	0.05	0.05	0.05	0.05	0.05	0.05	0.11	0.77	1.83	2.43	2.70	2.77	2.74	2.61	2.40	1.83	0.79	0.12	0.05	0.05	0.05	0.05
11	0.00	0.00	0.00	0.00	0.00	0.00	0.00	0.01	0.30	1.23	2.07	2.42	2.52	2.55	2.47	2.10	1.25	0.32	0.03	0.00	0.00	0.00	0.00	0.00
12	0.00	0.00	0.00	0.00	0.00	0.00	0.00	0.00	0.09	0.64	1.40	1.85	2.04	2.09	1.95	1.61	0.88	0.16	0.00	0.00	0.00	0.00	0.00	0.00

Average of q Column Labels																								
Month	**0**	**1**	**2**	**3**	**4**	**5**	**6**	**7**	**8**	**9**	**10**	**11**	**12**	**13**	**14**	**15**	**16**	**17**	**18**	**19**	**20**	**21**	**22**	**23**
1	1.13	1.12	1.10	1.09	1.09	1.09	1.09	1.08	1.09	1.08	1.06	1.03	1.02	1.02	1.03	1.04	1.06	1.08	1.12	1.17	1.19	1.18	1.17	1.14
2	1.22	1.21	1.20	1.18	1.17	1.15	1.15	1.15	1.17	1.14	1.08	1.03	1.01	1.02	1.04	1.07	1.09	1.10	1.11	1.16	1.21	1.25	1.25	1.25
3	1.38	1.35	1.31	1.30	1.27	1.25	1.25	1.25	1.26	1.23	1.16	1.12	1.12	1.14	1.15	1.17	1.19	1.22	1.23	1.24	1.28	1.34	1.38	1.39
4	1.19	1.18	1.16	1.15	1.15	1.14	1.13	1.13	1.12	1.07	1.05	1.09	1.13	1.16	1.19	1.22	1.23	1.23	1.22	1.19	1.14	1.15	1.18	1.19
5	1.01	1.01	0.99	0.98	0.96	0.95	0.96	0.95	0.91	0.87	0.89	0.91	0.93	0.95	0.95	0.94	0.94	0.93	0.94	0.94	0.93	0.91	0.95	1.00
6	1.01	1.02	1.01	0.98	0.94	0.92	0.90	0.88	0.80	0.73	0.74	0.78	0.84	0.88	0.91	0.95	0.98	0.99	0.99	0.95	0.90	0.86	0.90	0.97
7	0.70	0.72	0.73	0.71	0.70	0.68	0.67	0.64	0.56	0.45	0.42	0.45	0.48	0.51	0.54	0.57	0.58	0.58	0.56	0.53	0.48	0.48	0.55	0.63
8	0.77	0.78	0.78	0.76	0.74	0.72	0.70	0.69	0.66	0.55	0.47	0.48	0.51	0.54	0.56	0.56	0.57	0.56	0.56	0.52	0.50	0.56	0.66	0.74
9	1.08	1.07	1.05	1.02	1.01	0.99	0.97	0.96	0.94	0.85	0.76	0.77	0.80	0.84	0.87	0.90	0.91	0.90	0.87	0.81	0.84	0.95	1.04	1.08
10	1.14	1.12	1.11	1.10	1.10	1.10	1.10	1.11	1.11	1.09	1.03	1.01	1.04	1.06	1.09	1.11	1.12	1.11	1.06	1.01	1.05	1.11	1.15	1.16
11	1.28	1.27	1.25	1.24	1.23	1.23	1.22	1.22	1.22	1.18	1.12	1.09	1.10	1.12	1.15	1.16	1.15	1.14	1.17	1.23	1.27	1.29	1.30	1.29
12	1.21	1.19	1.17	1.15	1.13	1.13	1.12	1.12	1.13	1.13	1.08	1.01	0.98	0.98	0.99	1.00	1.01	1.04	1.13	1.20	1.24	1.26	1.26	1.25

Figure 13 Renewable electrical generation in MISO region, averaged month of year and hour of day (local timezone), normalized by overall average. Green and red represent higher and lower than average, respectively. Top: Solar photovoltaic. Bottom: wind. This is a simple estimate of periodic components of photovoltaic and wind electrical generation, and is used in to construct a nearly random time series that has the periodic components removed. The same information can be used as a two-dimensional lookup to generate a periodic time series with the same daily and seasonal behavior.

Average of qDemand	Column La										
Row Labels	**1**	**2**	**3**	**4**	**5**	**6**	**7**	**8**	**9**	**10**	**11**	**12**
0	0.94	0.90	0.83	0.79	0.82	0.97	1.04	0.99	0.89	0.81	0.83	0.91
1	0.92	0.88	0.81	0.77	0.79	0.92	0.98	0.94	0.85	0.78	0.81	0.88
2	0.91	0.87	0.80	0.75	0.76	0.88	0.94	0.90	0.82	0.76	0.80	0.86
3	0.90	0.86	0.79	0.74	0.74	0.85	0.91	0.88	0.80	0.75	0.79	0.86
4	0.90	0.86	0.79	0.74	0.73	0.83	0.88	0.86	0.78	0.74	0.79	0.85
5	0.90	0.87	0.80	0.74	0.73	0.82	0.87	0.85	0.78	0.74	0.79	0.86
6	0.92	0.88	0.81	0.75	0.73	0.81	0.87	0.85	0.78	0.75	0.81	0.87
7	0.94	0.90	0.83	0.76	0.73	0.81	0.87	0.85	0.79	0.77	0.83	0.89
8	0.97	0.93	0.85	0.78	0.76	0.85	0.90	0.88	0.81	0.79	0.86	0.92
9	0.99	0.95	0.87	0.81	0.80	0.91	0.97	0.93	0.86	0.82	0.88	0.94
10	1.00	0.95	0.88	0.83	0.84	0.97	1.04	1.00	0.91	0.84	0.89	0.96
11	0.99	0.95	0.88	0.84	0.86	1.02	1.10	1.06	0.95	0.86	0.89	0.95
12	0.99	0.94	0.88	0.84	0.89	1.07	1.16	1.12	1.00	0.87	0.89	0.95
13	0.98	0.94	0.87	0.84	0.91	1.10	1.20	1.16	1.03	0.89	0.88	0.94
14	0.97	0.93	0.87	0.84	0.92	1.13	1.24	1.20	1.06	0.89	0.88	0.94
15	0.96	0.93	0.86	0.84	0.93	1.15	1.27	1.22	1.08	0.90	0.88	0.93
16	0.97	0.93	0.86	0.84	0.94	1.16	1.29	1.24	1.10	0.91	0.88	0.94
17	0.99	0.95	0.87	0.85	0.95	1.18	1.30	1.26	1.11	0.92	0.92	0.98
18	1.04	0.98	0.89	0.86	0.96	1.18	1.31	1.26	1.11	0.93	0.97	1.03
19	1.06	1.01	0.91	0.87	0.96	1.17	1.29	1.24	1.09	0.95	0.97	1.04
20	1.06	1.01	0.94	0.88	0.94	1.14	1.25	1.21	1.09	0.96	0.96	1.03
21	1.04	0.99	0.94	0.90	0.95	1.12	1.22	1.20	1.07	0.94	0.94	1.01
22	1.01	0.96	0.91	0.87	0.93	1.09	1.19	1.14	1.01	0.90	0.91	0.98
23	0.97	0.93	0.87	0.83	0.87	1.03	1.12	1.08	0.95	0.85	0.87	0.94
24	0.96	0.90	0.84	0.80	0.82	0.95	1.05	1.01	0.90	0.81	0.84	0.90
25	0.94	0.88	0.82	0.77	0.79	0.91	0.99	0.96	0.86	0.79	0.82	0.87
26	0.93	0.87	0.81	0.76	0.76	0.87	0.95	0.93	0.83	0.77	0.81	0.86
27	0.93	0.87	0.81	0.75	0.75	0.85	0.92	0.90	0.81	0.76	0.81	0.86
28	0.94	0.88	0.81	0.76	0.74	0.84	0.91	0.90	0.81	0.77	0.82	0.86
29	0.96	0.90	0.83	0.78	0.76	0.85	0.92	0.91	0.82	0.79	0.84	0.88
30	1.01	0.96	0.89	0.83	0.79	0.88	0.95	0.95	0.86	0.84	0.90	0.94
31	1.09	1.04	0.97	0.90	0.84	0.93	0.99	1.00	0.91	0.92	0.98	1.01
32	1.12	1.07	1.00	0.93	0.88	0.99	1.05	1.05	0.94	0.96	1.02	1.05
33	1.12	1.07	1.01	0.95	0.92	1.05	1.12	1.10	0.98	0.97	1.02	1.05
34	1.12	1.07	1.01	0.96	0.95	1.09	1.18	1.16	1.02	0.98	1.02	1.05
35	1.11	1.06	1.01	0.96	0.98	1.14	1.24	1.22	1.07	1.00	1.02	1.05
36	1.10	1.05	1.00	0.96	1.00	1.18	1.30	1.27	1.11	1.01	1.01	1.04
37	1.08	1.04	0.99	0.96	1.02	1.21	1.34	1.32	1.15	1.02	1.00	1.03
38	1.07	1.04	0.99	0.97	1.03	1.24	1.38	1.35	1.18	1.03	1.00	1.02
39	1.06	1.03	0.98	0.96	1.04	1.26	1.40	1.37	1.20	1.03	0.99	1.01
40	1.06	1.02	0.97	0.96	1.05	1.26	1.41	1.37	1.21	1.03	0.99	1.01
41	1.08	1.03	0.97	0.96	1.05	1.26	1.41	1.37	1.21	1.03	1.01	1.04
42	1.13	1.06	0.98	0.96	1.05	1.26	1.40	1.36	1.20	1.03	1.05	1.09
43	1.14	1.09	0.99	0.96	1.04	1.24	1.38	1.34	1.18	1.04	1.06	1.09
44	1.13	1.09	1.01	0.96	1.02	1.20	1.34	1.30	1.17	1.04	1.04	1.08
45	1.10	1.06	1.00	0.97	1.02	1.17	1.30	1.27	1.14	1.01	1.02	1.06
46	1.06	1.02	0.97	0.94	0.99	1.14	1.25	1.21	1.08	0.96	0.98	1.03
47	1.02	0.97	0.92	0.88	0.93	1.07	1.17	1.13	1.01	0.91	0.93	0.98
48	0.98	0.94	0.88	0.84	0.87	0.99	1.09	1.06	0.94	0.87	0.89	0.94
49	0.96	0.92	0.86	0.81	0.83	0.94	1.03	1.01	0.90	0.83	0.86	0.92
50	0.95	0.90	0.84	0.79	0.80	0.90	0.98	0.96	0.87	0.81	0.85	0.90
51	0.94	0.90	0.84	0.78	0.78	0.87	0.95	0.94	0.85	0.80	0.84	0.90
52	0.95	0.90	0.84	0.78	0.78	0.86	0.93	0.92	0.84	0.80	0.84	0.90
53	0.96	0.92	0.86	0.80	0.79	0.87	0.94	0.93	0.85	0.81	0.86	0.92
54	1.02	0.97	0.91	0.84	0.83	0.89	0.97	0.97	0.90	0.86	0.92	0.97
55	1.10	1.05	0.98	0.91	0.89	0.94	1.01	1.02	0.97	0.94	0.99	1.04
56	1.13	1.08	1.01	0.94	0.93	0.99	1.07	1.06	1.00	0.97	1.02	1.08
57	1.13	1.07	1.01	0.95	0.96	1.04	1.13	1.10	1.03	0.98	1.02	1.08
58	1.12	1.07	1.01	0.95	0.99	1.09	1.19	1.16	1.07	0.99	1.02	1.07
59	1.11	1.06	1.00	0.96	1.02	1.13	1.25	1.21	1.12	1.01	1.02	1.06
60	1.10	1.05	0.99	0.96	1.04	1.17	1.30	1.26	1.16	1.02	1.01	1.05
61	1.08	1.04	0.99	0.96	1.06	1.21	1.35	1.30	1.19	1.03	1.01	1.03
62	1.07	1.04	0.98	0.96	1.07	1.24	1.38	1.34	1.22	1.04	1.00	1.02
63	1.06	1.03	0.97	0.96	1.08	1.25	1.40	1.36	1.24	1.04	1.00	1.02
64	1.06	1.02	0.96	0.96	1.09	1.26	1.42	1.37	1.25	1.04	1.00	1.02
65	1.08	1.03	0.96	0.96	1.09	1.27	1.42	1.37	1.25	1.04	1.02	1.05
66	1.13	1.06	0.97	0.96	1.08	1.26	1.41	1.35	1.23	1.04	1.05	1.10
67	1.14	1.09	0.99	0.95	1.07	1.23	1.38	1.32	1.21	1.05	1.06	1.10
68	1.13	1.08	1.01	0.96	1.05	1.20	1.34	1.28	1.20	1.05	1.04	1.09
69	1.11	1.06	1.01	0.97	1.04	1.17	1.30	1.26	1.17	1.02	1.02	1.07
70	1.07	1.02	0.97	0.94	1.01	1.14	1.26	1.20	1.10	0.98	0.98	1.04
71	1.03	0.98	0.92	0.89	0.95	1.07	1.18	1.12	1.03	0.92	0.93	0.99
72	0.99	0.94	0.89	0.84	0.89	0.99	1.10	1.05	0.96	0.87	0.89	0.96
73	0.97	0.92	0.87	0.81	0.84	0.94	1.03	0.99	0.92	0.83	0.87	0.93
74	0.96	0.91	0.85	0.79	0.82	0.90	0.99	0.95	0.88	0.81	0.85	0.91
75	0.96	0.90	0.84	0.78	0.80	0.87	0.95	0.92	0.86	0.80	0.84	0.90
76	0.96	0.91	0.84	0.78	0.79	0.86	0.94	0.91	0.85	0.80	0.84	0.91
77	0.98	0.93	0.86	0.80	0.80	0.87	0.94	0.92	0.86	0.81	0.86	0.92
78	1.03	0.98	0.91	0.84	0.84	0.89	0.97	0.96	0.91	0.86	0.91	0.97
79	1.11	1.06	0.99	0.90	0.89	0.94	1.01	1.00	0.97	0.93	0.99	1.05
80	1.14	1.09	1.02	0.93	0.94	0.99	1.07	1.04	1.00	0.97	1.02	1.08
81	1.13	1.08	1.01	0.94	0.96	1.04	1.13	1.09	1.03	0.98	1.02	1.08
82	1.12	1.08	1.01	0.95	0.99	1.09	1.19	1.14	1.07	0.99	1.02	1.07
83	1.11	1.07	1.00	0.95	1.01	1.13	1.25	1.19	1.11	1.00	1.02	1.06
84	1.09	1.06	0.99	0.95	1.03	1.17	1.31	1.24	1.14	1.01	1.01	1.05
85	1.08	1.05	0.98	0.95	1.05	1.21	1.35	1.28	1.18	1.02	1.00	1.03
86	1.07	1.04	0.98	0.96	1.07	1.24	1.39	1.32	1.21	1.04	1.00	1.03
87	1.06	1.03	0.97	0.95	1.08	1.26	1.41	1.34	1.22	1.04	1.00	1.02
88	1.06	1.03	0.96	0.95	1.08	1.27	1.42	1.35	1.23	1.04	0.99	1.02
89	1.08	1.04	0.96	0.95	1.08	1.26	1.42	1.35	1.23	1.04	1.01	1.05
90	1.12	1.07	0.97	0.95	1.08	1.25	1.41	1.34	1.22	1.04	1.05	1.10
91	1.14	1.11	0.99	0.95	1.06	1.24	1.38	1.31	1.19	1.05	1.05	1.11
92	1.13	1.10	1.01	0.95	1.04	1.21	1.34	1.27	1.18	1.05	1.03	1.09
93	1.11	1.08	1.00	0.97	1.04	1.17	1.30	1.25	1.15	1.02	1.01	1.07
94	1.07	1.04	0.96	0.93	1.01	1.14	1.25	1.19	1.09	0.97	0.97	1.04
95	1.02	0.99	0.92	0.88	0.95	1.07	1.18	1.11	1.01	0.92	0.92	0.99
96	0.99	0.96	0.88	0.84	0.89	0.99	1.10	1.04	0.96	0.86	0.88	0.95
97	0.97	0.94	0.85	0.81	0.85	0.94	1.04	0.98	0.92	0.83	0.85	0.92
98	0.95	0.93	0.84	0.79	0.82	0.90	0.99	0.94	0.88	0.81	0.83	0.91
99	0.95	0.92	0.83	0.78	0.80	0.87	0.96	0.92	0.86	0.79	0.83	0.90
100	0.95	0.93	0.83	0.78	0.79	0.86	0.94	0.91	0.85	0.79	0.82	0.90
101	0.97	0.95	0.85	0.79	0.81	0.87	0.95	0.91	0.86	0.81	0.84	0.92
102	1.02	1.00	0.90	0.84	0.84	0.90	0.97	0.95	0.91	0.86	0.88	0.97
103	1.10	1.08	0.98	0.90	0.90	0.94	1.02	1.00	0.97	0.93	0.95	1.04
104	1.14	1.11	1.01	0.93	0.94	0.99	1.07	1.04	1.00	0.96	0.98	1.08
105	1.13	1.10	1.01	0.94	0.97	1.04	1.13	1.08	1.03	0.97	0.98	1.08
106	1.12	1.09	1.00	0.95	1.00	1.09	1.19	1.13	1.07	0.98	0.99	1.07
107	1.10	1.08	1.00	0.95	1.02	1.14	1.25	1.19	1.11	1.00	0.99	1.07
108	1.09	1.07	0.99	0.95	1.04	1.18	1.31	1.23	1.15	1.01	0.98	1.05
109	1.07	1.06	0.98	0.95	1.06	1.21	1.35	1.27	1.18	1.01	0.97	1.04
110	1.06	1.05	0.98	0.95	1.07	1.25	1.39	1.31	1.21	1.02	0.97	1.03
111	1.05	1.04	0.97	0.94	1.08	1.27	1.41	1.33	1.23	1.02	0.96	1.02
112	1.05	1.04	0.96	0.94	1.08	1.28	1.42	1.34	1.23	1.02	0.95	1.03
113	1.07	1.05	0.96	0.94	1.08	1.29	1.42	1.34	1.23	1.02	0.97	1.06
114	1.11	1.08	0.97	0.94	1.08	1.28	1.41	1.33	1.22	1.02	1.00	1.10
115	1.13	1.11	0.99	0.94	1.06	1.25	1.38	1.30	1.19	1.03	1.01	1.10
116	1.12	1.11	1.00	0.94	1.04	1.22	1.34	1.26	1.18	1.04	0.99	1.09
117	1.10	1.09	1.00	0.96	1.04	1.19	1.30	1.24	1.16	1.01	0.97	1.07
118	1.06	1.06	0.96	0.92	1.01	1.15	1.25	1.19	1.09	0.96	0.94	1.04
119	1.02	1.01	0.91	0.87	0.95	1.08	1.18	1.11	1.02	0.91	0.90	0.99
120	0.97	0.98	0.88	0.83	0.87	1.01	1.10	1.04	0.95	0.86	0.87	0.95
121	0.95	0.96	0.86	0.80	0.83	0.96	1.03	0.99	0.91	0.83	0.84	0.93
122	0.94	0.95	0.84	0.79	0.80	0.91	0.98	0.95	0.87	0.80	0.83	0.91
123	0.93	0.95	0.84	0.78	0.79	0.89	0.95	0.92	0.85	0.79	0.82	0.90
124	0.93	0.95	0.84	0.77	0.78	0.87	0.93	0.91	0.84	0.79	0.82	0.90
125	0.95	0.97	0.85	0.79	0.79	0.88	0.94	0.91	0.85	0.80	0.84	0.92
126	1.00	1.02	0.90	0.83	0.82	0.90	0.96	0.95	0.89	0.85	0.88	0.97
127	1.07	1.10	0.97	0.89	0.87	0.94	1.00	0.99	0.96	0.92	0.95	1.04
128	1.11	1.13	1.00	0.92	0.92	1.00	1.05	1.03	0.99	0.95	0.97	1.07
129	1.11	1.12	1.00	0.93	0.95	1.06	1.12	1.08	1.02	0.96	0.98	1.08
130	1.10	1.11	1.00	0.94	0.97	1.11	1.18	1.13	1.06	0.98	0.98	1.07
131	1.09	1.09	1.00	0.94	0.99	1.16	1.24	1.18	1.09	0.99	0.98	1.06
132	1.08	1.07	0.98	0.94	1.01	1.21	1.29	1.22	1.13	0.99	0.97	1.05
133	1.07	1.06	0.97	0.94	1.02	1.24	1.33	1.26	1.16	1.00	0.97	1.03
134	1.05	1.04	0.96	0.94	1.03	1.27	1.37	1.30	1.18	1.00	0.96	1.02
135	1.04	1.03	0.95	0.93	1.03	1.29	1.39	1.32	1.20	1.00	0.95	1.01
136	1.04	1.02	0.94	0.92	1.03	1.30	1.40	1.32	1.20	0.99	0.95	1.01
137	1.05	1.02	0.94	0.92	1.03	1.30	1.40	1.32	1.19	0.99	0.97	1.04
138	1.09	1.05	0.94	0.91	1.02	1.29	1.38	1.30	1.17	0.98	0.99	1.08
139	1.10	1.08	0.96	0.90	1.00	1.26	1.35	1.27	1.14	0.99	0.99	1.08
140	1.08	1.07	0.97	0.91	0.98	1.22	1.30	1.22	1.12	0.98	0.98	1.06
141	1.06	1.06	0.96	0.92	0.98	1.18	1.25	1.20	1.09	0.96	0.96	1.04
142	1.03	1.03	0.94	0.90	0.95	1.15	1.21	1.15	1.04	0.92	0.93	1.01
143	0.99	0.99	0.90	0.86	0.90	1.08	1.14	1.08	0.98	0.88	0.89	0.97
144	0.96	0.96	0.86	0.82	0.85	1.01	1.07	1.01	0.93	0.84	0.86	0.94
145	0.94	0.94	0.84	0.79	0.81	0.95	1.01	0.96	0.89	0.80	0.83	0.91
146	0.92	0.92	0.82	0.77	0.78	0.90	0.96	0.92	0.85	0.78	0.82	0.89
147	0.92	0.91	0.81	0.76	0.76	0.87	0.93	0.89	0.83	0.77	0.81	0.88
148	0.92	0.91	0.81	0.76	0.75	0.85	0.90	0.87	0.81	0.76	0.81	0.88
149	0.92	0.92	0.82	0.76	0.75	0.85	0.89	0.87	0.81	0.77	0.81	0.88
150	0.94	0.94	0.84	0.78	0.76	0.85	0.89	0.88	0.82	0.78	0.83	0.90
151	0.97	0.97	0.86	0.79	0.76	0.86	0.90	0.88	0.84	0.81	0.86	0.93
152	1.00	1.00	0.89	0.82	0.79	0.90	0.94	0.91	0.86	0.84	0.89	0.96
153	1.02	1.01	0.91	0.85	0.84	0.96	1.00	0.97	0.90	0.87	0.91	0.99
154	1.03	1.02	0.92	0.86	0.87	1.02	1.07	1.03	0.95	0.89	0.92	1.00
155	1.03	1.01	0.92	0.87	0.90	1.07	1.14	1.08	0.99	0.90	0.92	0.99
156	1.01	0.99	0.91	0.87	0.92	1.12	1.19	1.13	1.03	0.91	0.92	0.98
157	1.00	0.97	0.90	0.87	0.93	1.15	1.23	1.17	1.06	0.91	0.91	0.97
158	0.98	0.95	0.89	0.86	0.94	1.17	1.26	1.20	1.08	0.91	0.90	0.95
159	0.97	0.94	0.88	0.85	0.94	1.19	1.28	1.22	1.09	0.91	0.89	0.95
160	0.97	0.94	0.88	0.85	0.95	1.21	1.29	1.23	1.10	0.91	0.89	0.95
161	0.99	0.95	0.88	0.86	0.96	1.22	1.30	1.24	1.11	0.91	0.91	0.98
162	1.04	0.98	0.89	0.86	0.96	1.22	1.30	1.24	1.10	0.92	0.95	1.03
163	1.05	1.01	0.91	0.86	0.95	1.20	1.27	1.21	1.07	0.93	0.96	1.03
164	1.04	1.00	0.92	0.87	0.93	1.16	1.23	1.17	1.06	0.93	0.94	1.01
165	1.03	0.99	0.92	0.88	0.93	1.13	1.19	1.15	1.04	0.91	0.93	1.00
166	1.00	0.96	0.90	0.86	0.91	1.10	1.16	1.11	0.99	0.88	0.90	0.98
167	0.97	0.93	0.86	0.83	0.87	1.04	1.10	1.04	0.94	0.84	0.87	0.94

Figure 14 Electrical demandin MISO region, averaged for month of year and hour of week (local timezone), normalized by overall average. Green and red represent higher and lower than average, respectively. This is a simple estimate of periodic components of, and is used in to construct a nearly random time series that has the periodic components removed. The same information can be used as a two-dimensional lookup to generate a periodic time series with the same daily, weekly, and seasonal behavior.

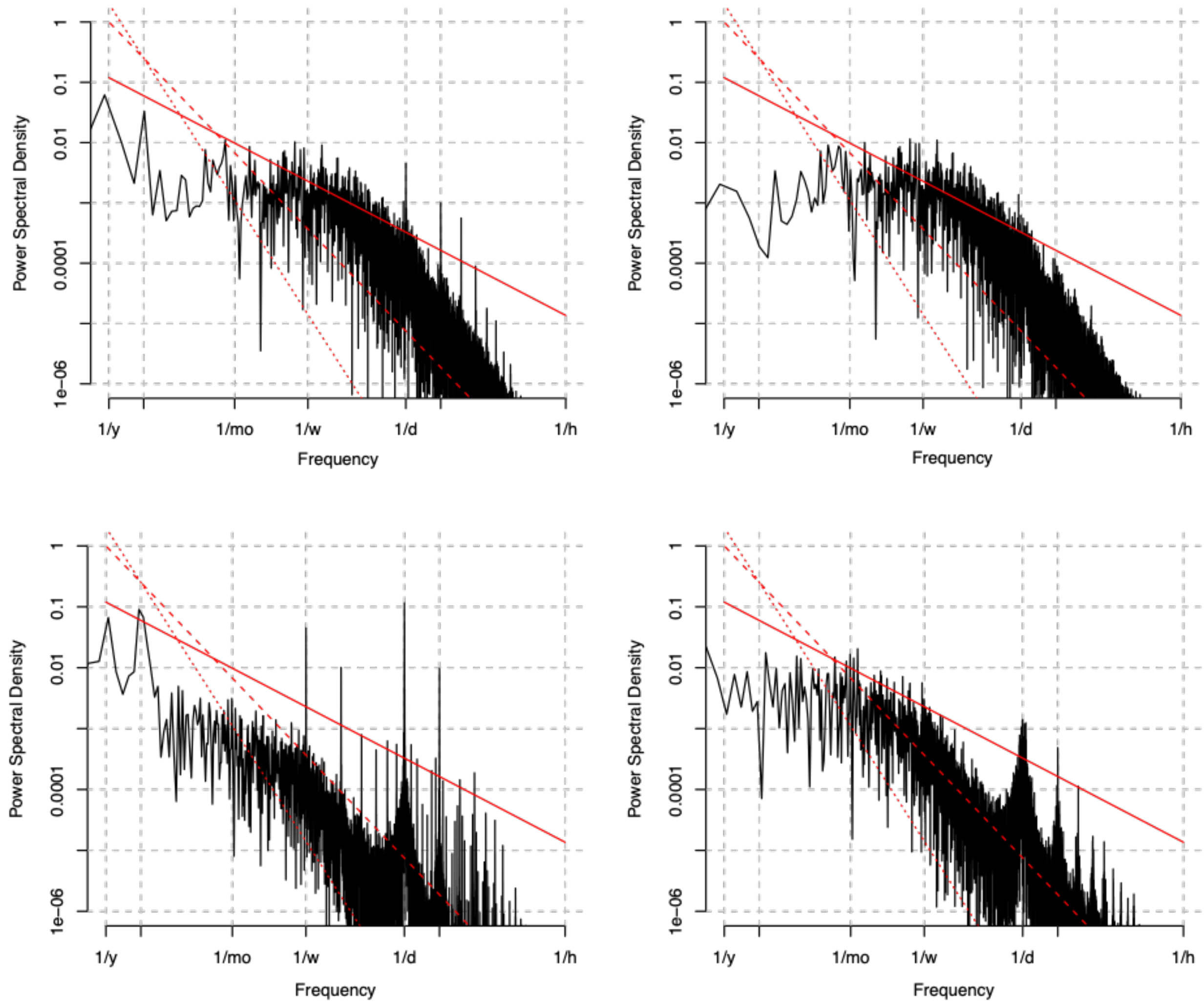

Figure 15 *Power spectral density of wind (top) demand (bottom), both before (left) and after (right) removal of the periodic components. Power spectral density of wind and demand can be well-represented by a Markov- Gauss process with timescales of one week and one month respectively.*